Particle Accelerators, 1972, Vol. 4, pp. 87–99

HIGH GRADIENT PRECISION QUADRUPOLE MAGNETS FOR KEK LINEAR ACCELERATOR

M. KOBAYASHI, J. TANAKA, H. BABA, S. INAGAKI AND S. OKUMURA
National Laboratory for High Energy Physics, Oho-machi, Tsukuba-gun, Ibaraki, Japan

AND

S. YAMASHITA
Department of Physics, Nara Women's University, Nara, Japan

New manufacturing processes of drift tube quadrupole magnets were developed to obtain a high field gradient of 11 kG/cm and a high mechanical precision. A total of 90 magnets for the KEK linac were constructed with a tolerance of 20 μm for the difference between the mechanical bore centres and the magnetic centres. The field characteristics, i.e., core saturation, fringing field distribution, effective length of magnet, harmonic contents and eddy current effects, were measured in pulsed excitation with a new measuring system using a peak-to-dc comparison method and a stepping search coil.

1. INTRODUCTION

Pulsed quadrupole magnets[1] having a high field gradient and a high mechanical precision were developed for the 20 MeV linac[2] of KEK (National Laboratory for High Energy Physics in Japan) Proton Synchrotron.

The high field gradient was achieved by the use of narrow rectangular coil slots with machined coils. The circular profile of the pole tip was determined by a numerical calculation[3] to make non-linear fields small.

The high mechanical precision was achieved by a quality control of manufacturing processes of punching of core leaves, stacking and assembling of the cores. Prior to manufacturing, various tests[4] were made for these processes in order to establish the best construction method. Performance of different methods for each process was inspected for both mechanical and magnetic properties.

The quadrupole magnets will be used under a pulsed excitation at a repetition of 20 pps with the pulse shape of approximately a half sinusoid (see Fig. 1).

In order to determine the saturation and eddy current effects, it is desirable to examine the magnetic properties under the actual condition of pulsed excitation. So far, there has been no adequate method for precise measurement of the pulsed fields in the present frequency range. We have completed a comprehensive system of field measurement, by which both dc and pulsed fields can be measured with only a slight modification of the apparatus. The constructed quadrupole magnets were examined for the field characteristics, i.e., saturation, fringing field distribution, effective length of magnet, harmonic contents and eddy current effects.

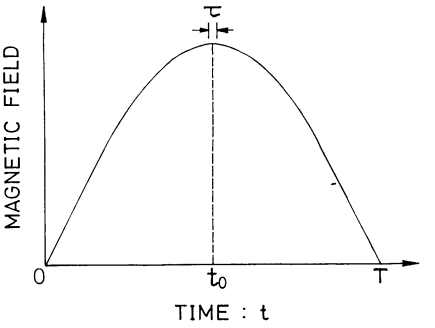

FIG. 1. Pulse shape of magnetic field. T is around 1.3 msec. The pulsed power supply is now being changed to produce a flat top of 0.1 per cent flatness during 120 μsec at t_0. In actual operation of the linac in future, this modified pulse shape will be used.

In this paper are described the magnet design in Sec. 2, the construction method together with the performance in Sec. 3, and the measurement of the field distributions in Sec. 4.

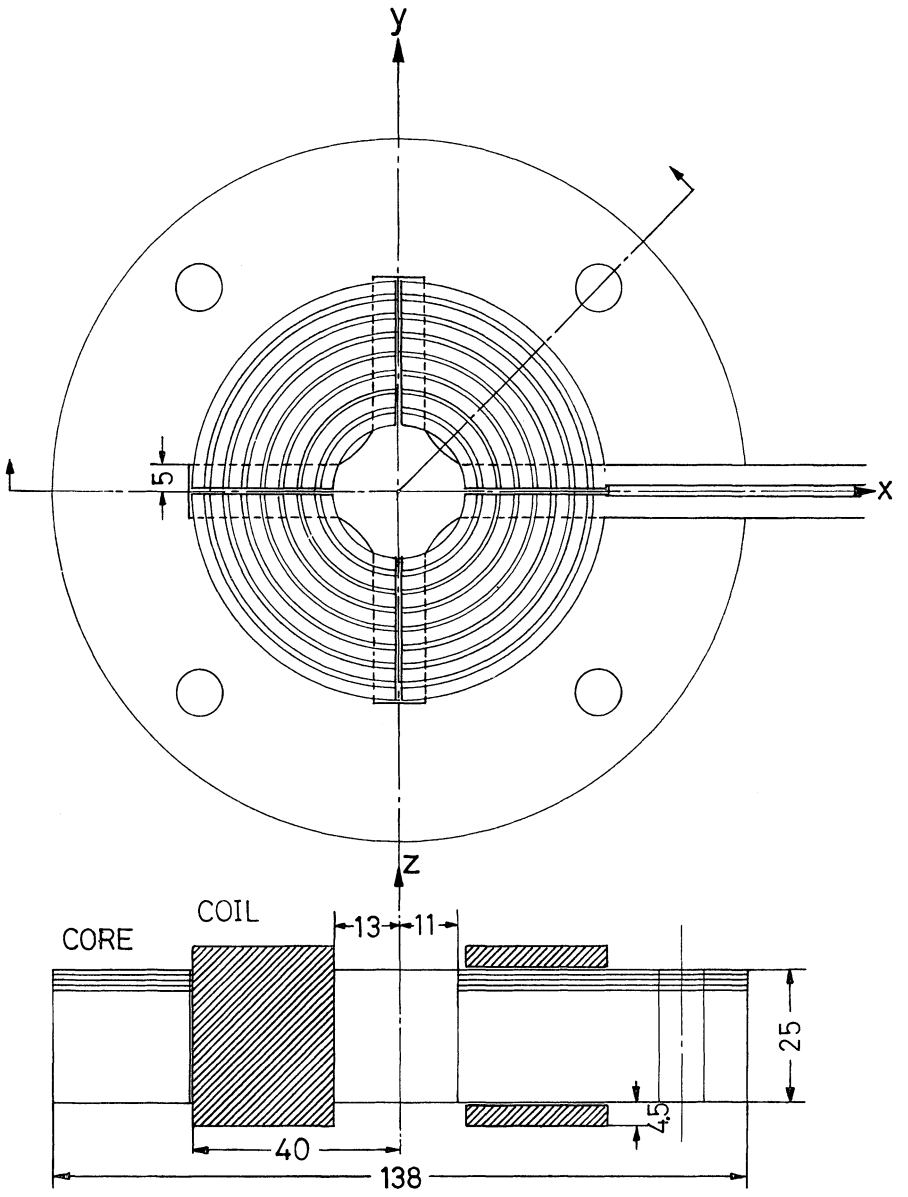

FIG. 2. Dimension of a QM25 quadrupole magnet.

2. DESIGN

In Fig. 2 are given the dimensions of the quadrupole magnet used at the 0.75 MeV injection end of the linac. The total of 90 magnets is divided into five groups, with core thicknesses of 25 mm (magnet designated QM25), 35 mm (QM35), 50 mm (QM50), 75 mm (QM75), and 100 mm (QM100). Corresponding to the change of the bore diameter at drift tube No. 28 from 20 mm to 25 mm, there are two different pole profiles A and B (see Fig. 3).

A complete magnet consists of four separate quadrant cores. Core leaves were punched from a cold-rolled silicon steel sheet of 0.35 mm thickness.

A complete coil consists of four quadrant coils. A quadrant coil was shaped from a copper block by machining (see Fig. 4) and has 7.5 turns. The turn-to-turn and coil-to-core insulation was made by inserting sheets of phenol resin. Four quadrant coils were assembled into a complete unit on a jig and impregnated with epoxy resin. A cooling

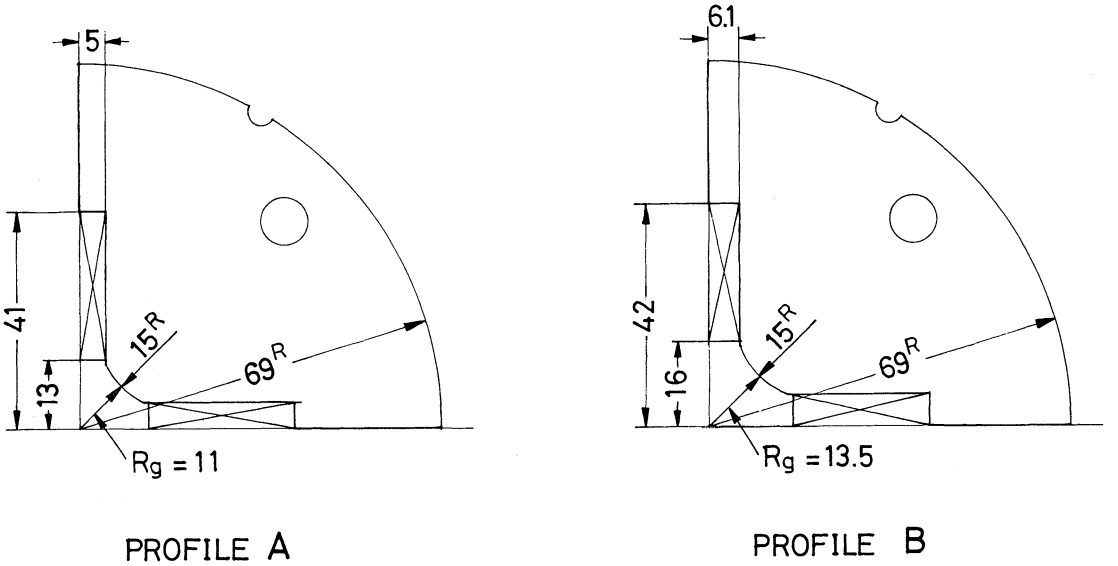

FIG. 3. Two profiles A and B of punched core leaves.

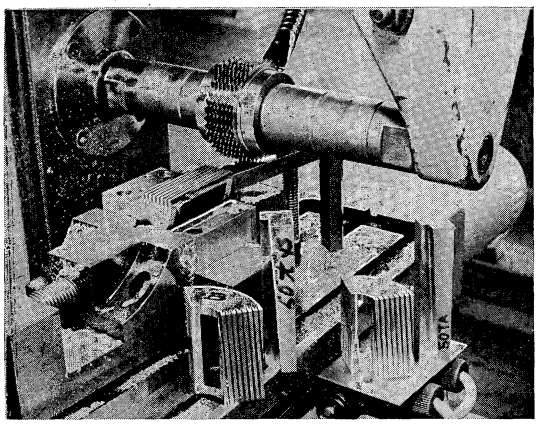

FIG. 4. Machining a quadrant unit of cut coil. Grooves are cut in the side surfaces and then in the end surfaces.

water channel is mounted on the outer periphery of the magnet (see Figs. 5 and 6).

3. CONSTRUCTION

For the construction of a precise magnet core, the most important two requirements are the following:

(1) the relative positions of the four poles should be symmetrical and each pole should be symmetrical about the 45° axis of the quadrant,

(2) the magnetic centre should coincide with the mechanical centre of bore tube.

In order to satisfy these requirements, we have adopted a tight control[5] of magnet manufacturing processes of punching of core leaves, stacking and assembling of the cores.

Punching

The highest accuracy was required for the set of punch and die at the gap radius, the pole tip profile and the butting surfaces between the quadrants. The dimension of punched core leaves coincided with that of the die within 5 μm and the maximum deviation among many core leaves were less than ± 2 μm. The maximum left and right symmetry error of a punched core leaf was less than 8 μm.

Stacking

In the stacking process, the following three requirements have to be satisfied:

(1) accurate outer dimension and the left and right symmetry of the core cross section,
(2) no tilting with respect to the end plane,
(3) uniform core thickness.

Core leaves were stacked on a jig (Fig. 7) with the right side in the same direction without filing off the punching burrs. The jig has a rigid structure

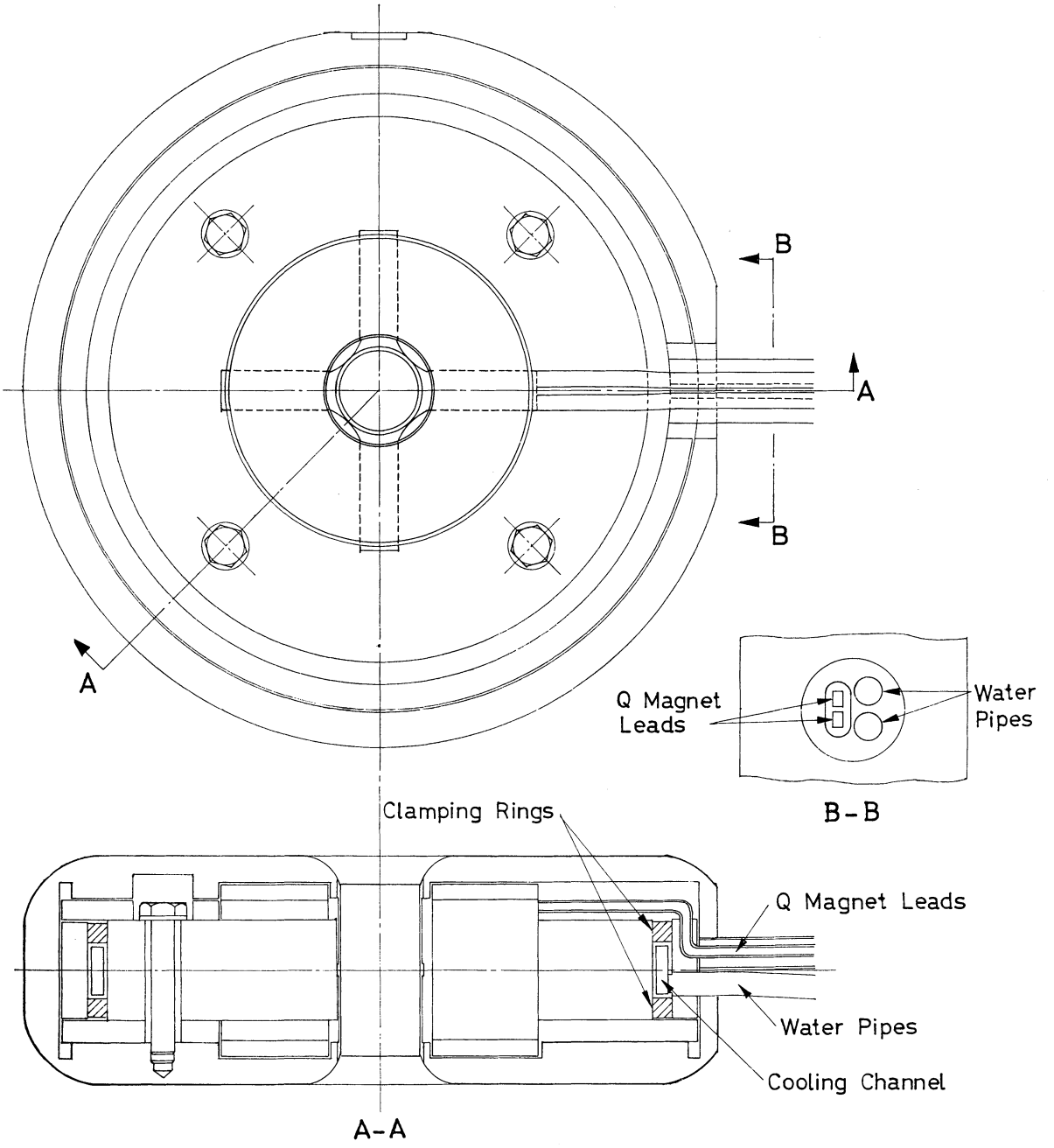

FIG. 5. A sketch of a QM25 quadrupole magnet mounted in a drift tube.

of square blocks as the reference of position. The epoxying procedure was as follows: stacking core leaves on a jig, painting epoxy resin on the periphery, wiping off superfluous epoxy resin from the painted surfaces, curing in a furnace, demounting the core from the stacking jig, and finally scraping off the hardened superfluous epoxy from the painted surfaces. With this stacking scheme, core thickness was uniform within ± 15 μm.

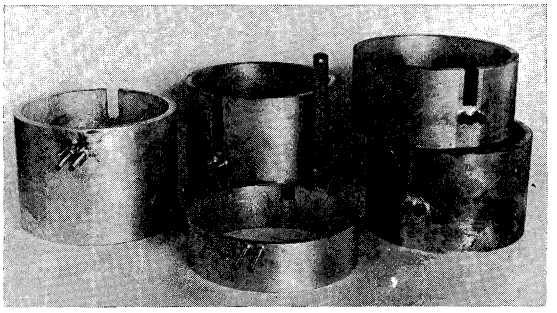

Fig. 6. Water jackets of various lengths. The inside is divided into several compartments and water flows through them in series so as to increase cooling efficiency.

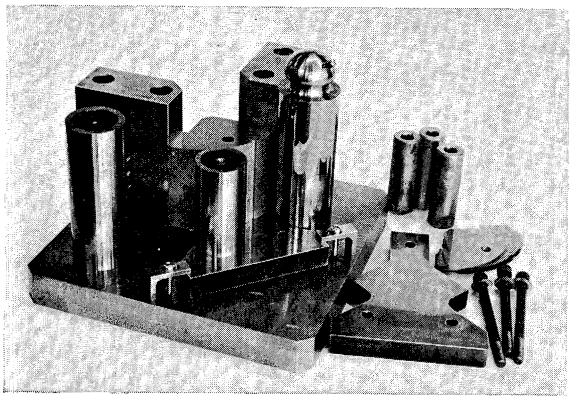

FIG. 7. Stacking process.

Assembling

Two diagonal quadrant cores were first bolted to the assembling jig with contact between the straight edges of the yokes and the reference blocks (Fig. 8). The reference blocks were then replaced by the other two quadrant cores which were then bolted down.

Then the four quadrant cores were clamped together by shrinking an aluminum ring around the assembly. The photograph in Fig. 9 illustrates the method of fitting the shrunk ring. This clamping method has an advantage that the strong shrinking pressure improves the symmetry of four quadrants in position.

Deviation of the outer surface of the magnet from a complete circle was as small as ~ 10 μm. The magnet outer surface was completely cylindrical within 5 μm.

Corresponding to different magnet lengths, various shrunk rings were used. For QM25, two rings, each 5 mm thick and 5 mm high, were tightened with a shrinkage allowance of ~ 0.15 mm. The shrinking pressure averaged over the magnet outer surface was 13 kg/cm^2. Shrinkage of core was found to be 0.02 ± 0.01 mm in the gap distance.

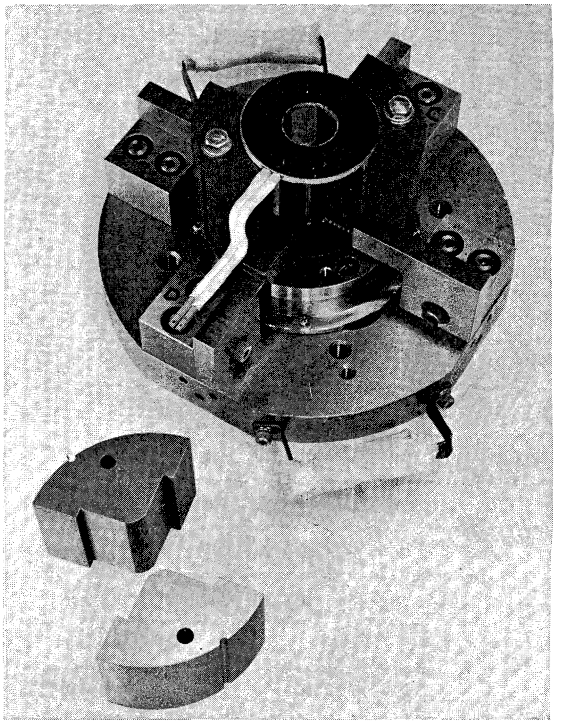

FIG. 8. Assembling process.

Fitting a Bore Tube

In order to facilitate the alignment of magnets in the linac tank, the mechanical centre of the magnet should coincide with the centre of the bore tube. The gap between opposite pole tips was used as a reference for centring. Then a bore tube was pressed into the minimum gap with a negligible

clearance. This method has a merit that at a relatively high operating temperature the magnet core cannot drift away in position with respect to the bore tube.

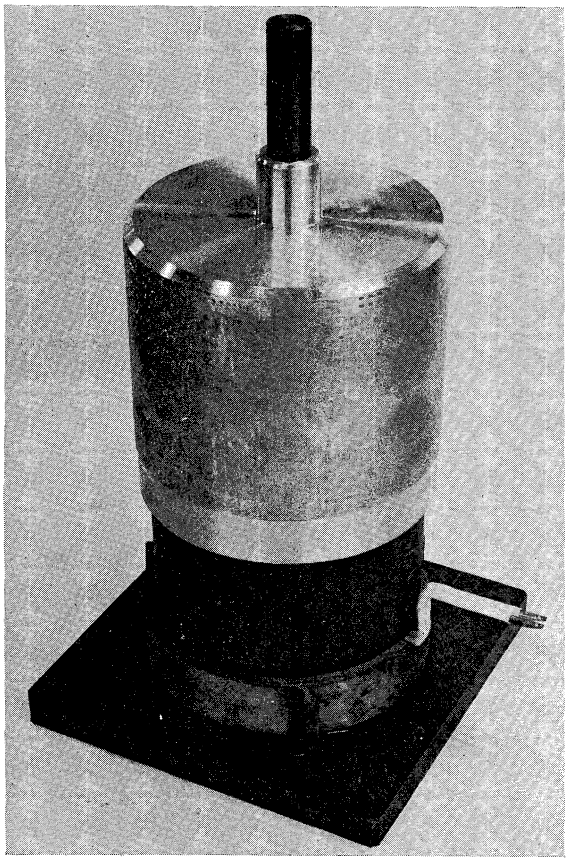

FIG. 9. Procedure of fitting shrunk rings.

Coil

The coil has a simple structure and can be machined to precise dimensions. Turn-to-turn short circuits were checked by measuring the inductance and Q-value of the coil without core by a Q-meter. The measurement was made at a resonant frequency around a few MHz with a Q-value of more than several tens. The inductance of each coil was distributed within ± 2 per cent and the error in measurement was less than 0.1 per cent. One turn short circuited caused a decrease of inductance by about 12 per cent and of the Q-value by about half. Short circuits due to a lightly touching metal chip only caused a decrease of the Q-value without a change in inductance. As a result, turn-to-turn short circuits are easily detectable.

Performance

All magnets for the linac have been constructed at the manufacturers. A photograph of assembled magnet QM25 is shown in Fig. 10. A series of mechanical, electrical and magnetic checks were made on each magnet. The most critical check was made about the deviation of the magnetic centre from the mechanical centre, which was determined at the centre of a bore tube fit into the minimum gap. The small deviation is essential for a negligibly small dipole field component. The rms deviations of the magnetic centres from the mechanical centres were 12 μm for QM25 (number of magnets being 8), 7 μm for QM35 (8), 14 μm for QM50 (16), 14 μm for QM75 (24) and 12 μm for QM100 (34), which are well within the tolerance value of 20 μm.

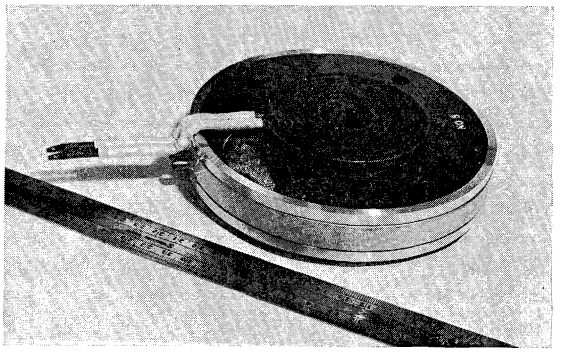

FIG. 10. A completed quadrupole magnet of QM25.

The minimum gap distance was identical for magnets of the same group, being measured with cylinder gauges whose step is 20 μm. A bore tube of the fixed outer diameter was pressed into the pole gap with a negligibly small clearance by a force of a few kilograms.

The magnet was installed into a drift tube with the tolerance of 2 μm for parallelism between the magnet end plane and the drift tube end plane, and 2.5 mrad for azimuthal position of magnet. The bore tube was fixed at right angle to the magnet end plane within 0.1 mrad.

After closing the drift tube by electron beam welding, the space around the magnet was impreg-

nated in vacuum with an epoxy resin containing 28 per cent of alumina powder by weight.

4. MEASUREMENT OF MAGNETIC FIELDS

Magnetic field was measured for both dc and pulsed excitation of the magnet.

Dc field was measured by using a rotating search coil.[6] A quadrupole magnet and a search coil were mounted on a precision testing apparatus of magnets called a centering machine.[6] The emf induced in the search coil was fed to a wave analyzer through a slip-ring and brush assembly to obtain the harmonic field content. The sensitivity for the magnetic centre location was within 0.5 μm and the reproducibility within ± 2 μm. Harmonic field content was obtained usually with an accuracy of ± 5 per cent, the accuracy depending on that of the wave analyzer.

Pulsed field was measured at the peak field (at the instant t_0: see Fig. 1) by a peak-to-dc comparison method[7] for the excitation pulse with $T \sim 4.5$ msec. As a beam pulse has a short duration of $\tau \simeq 20$ μsec at the time t_0, the magnetic field of interest is the peak field.

The emf induced in a stationary search coil by a pulsed field, is electronically integrated. The integrator's output $F(t)$ is compared at the time t_0 with an adjustable dc reference voltage V_r by using a cathode ray oscilloscope as a null indicator. If V_r is adjusted so that $F(t_0)+V_r$ coincides with the ground level, $-V_r$ gives $F(t_0)$. With the present measuring system,[7] $F(t_0)$ below several volts was measured with an accuracy of 0.1 mV.

For measurement of the harmonic content of pulsed magnets, a Fourier analysis method was developed[8] using a stepping search coil. A search coil was rotated step by step by a fixed step angle of arbitrary multiples of one degree. A set of precision worm and worm wheel was used for step-driving the search coil. Harmonic field content was found by Fourier—analyzing a set of magnetic

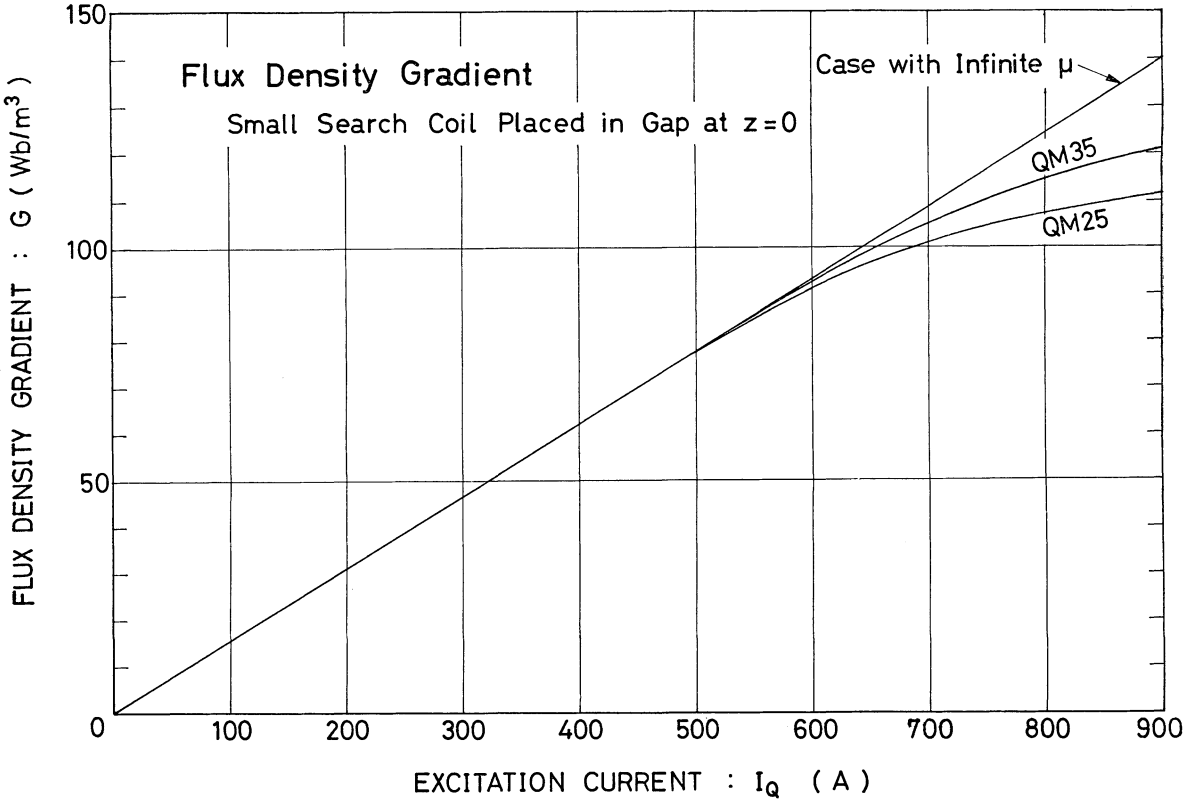

FIG. 11. The flux density gradients obtained in QM25 and QM35.

fluxes obtained at different angular positions of the search coil. The position of magnetic centre could be obtained using the result of Fourier analysis. Accuracy of obtained harmonic content, in terms of the ratio of harmonic components at the gap radius $(B_n/B_2)_{R_g}$, was as high as 1×10^{-4} for the components of $n \leqq 10$. The measurements of the magnetic centre were reproducible within 2 μm.

Excitation

In Fig. 11 are presented the excitation characteristics of QM25 and QM35. The field gradient of 11 kG/cm was obtained by QM25. For QM35, it was increased to 12 kG/cm because of the relatively small amount of fringing field which escapes from the core region towards the outside. In Fig. 12 are presented excitation curves obtained at different positions on the axis. The effect of saturation is largest at about 5 mm outside the core end plane.

Fringing Field

Fringing field distributions on the axis are given in Fig. 13 for different values of excitation current. The distribution in the fringing region was almost the same for QM25 and QM35. Effective magnet length was obtained by graphically integrating the fringing field distribution and is given in Fig. 14. Half of the difference between the effective and mechanical lengths is about 20 per cent of the gap diameter $2R_g$, and shows a slight decrease as the excitation current increases.

Fringing field distribution of each harmonic component is presented in Fig. 15 for the second, the sixth and the tenth components. The sixth component has two peaks at both of the magnet

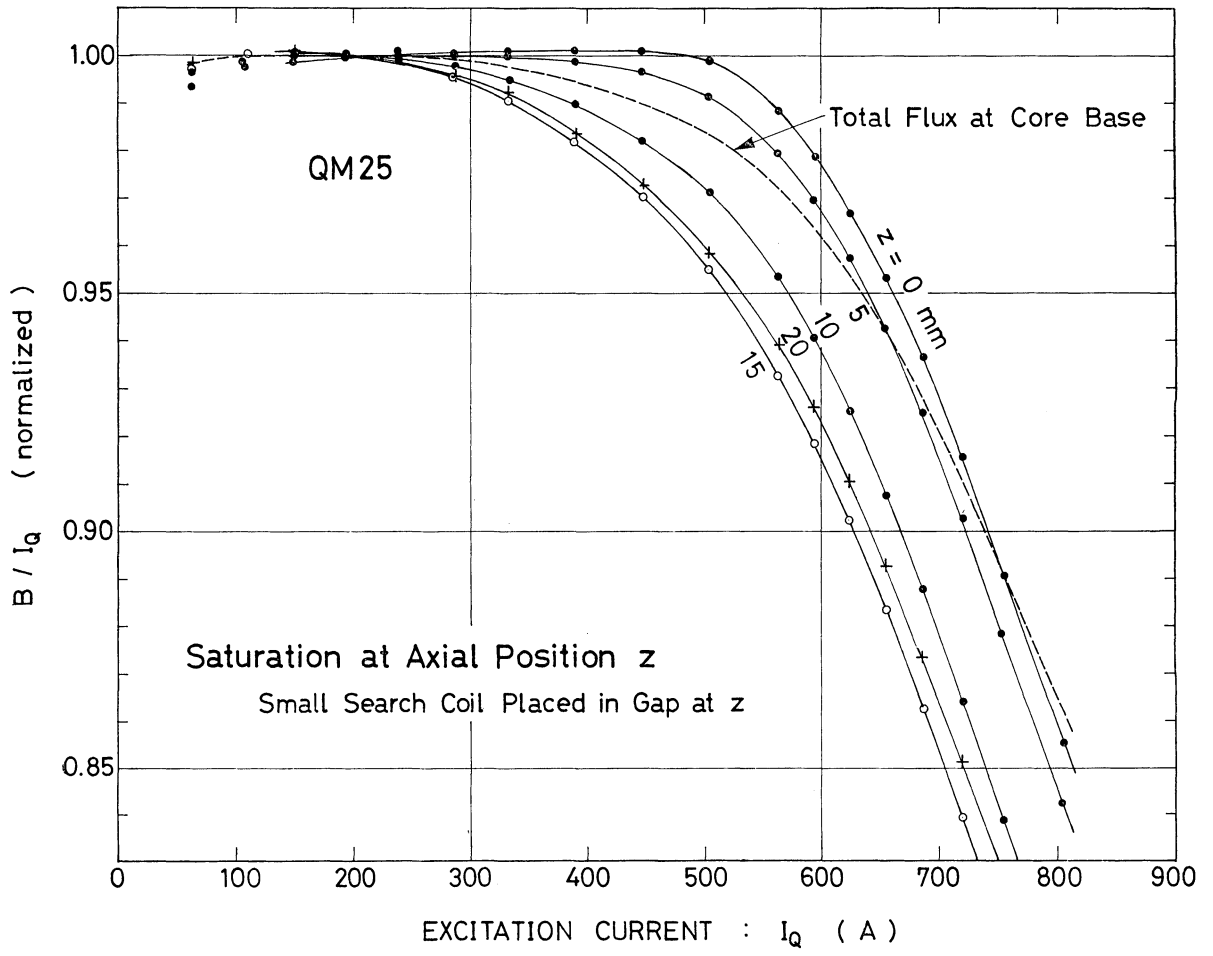

Fig. 12(a)

ends on the axis. The distribution of the tenth component is similar to that of the quadrupole component except that it has a more rapid fall with the axial distance from the median plane.

Harmonic Contents[8]

Harmonic contents at the gap radius measured with a long search coil (length = 55 mm) were representatively as follows; $(B_n/B_2)_{R_g} \simeq 3.9$ per cent for $n = 6$ and 2.8 per cent for $n = 10$ for the pole profile A, and $\simeq 3.5$ per cent for $n = 6$ and 4.0 per cent for $n = 10$ for the pole profile B. The other nonlinear components with $n = 3 \sim 5$ and $7 \sim 9$ were as small as 0.1 per cent of the main quadrupole component except for the component of $n = 4$ of roughly 0.3 per cent.

A rather large octupole term ($n = 4$) is expected to be due to a left and right asymmetry of the coil about the 45° axis of the quadrant. The coil is symmetrical for the azimuthal rotation of $\pi/2$ while any quadrant coil is asymmetrical about the 45° axis of the quadrant because of the last half turn lying nearest the magnet centre. The octupole term of each magnet will be of almost the same magnitude with the polarity determined by the direction of the excitation current. Consequently, the effect of the octupole term on the beam will be qualitatively focusing similarly to that of the quadrupole term and not so harmful.

A measured dependence of harmonic contents on excitation current is presented in Fig. 16. No deterioration of the field quality was found for the

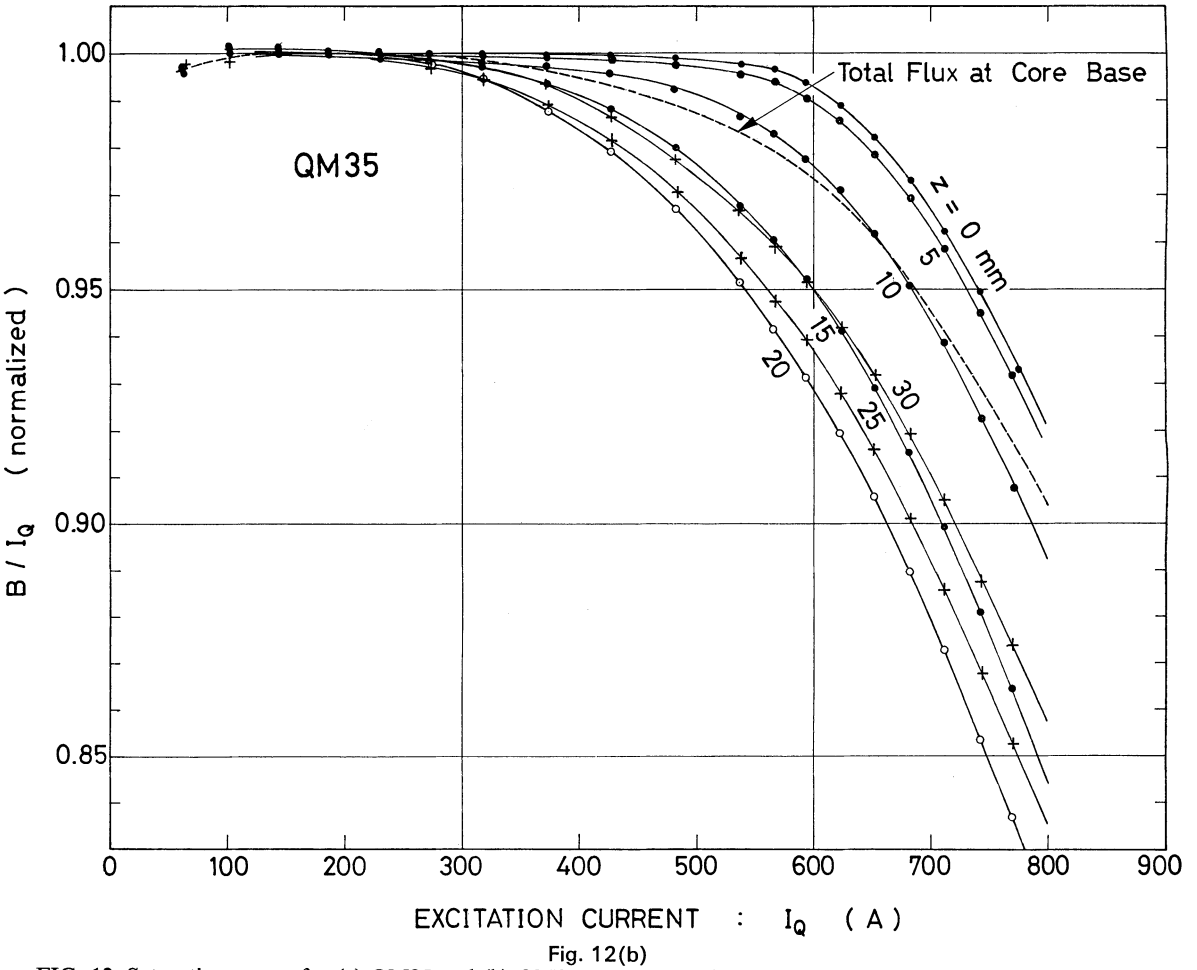

Fig. 12(b)

FIG. 12. Saturation curves for (a) QM25 and (b) QM35 at various axial positions z, whose zero is set at the magnet centre.

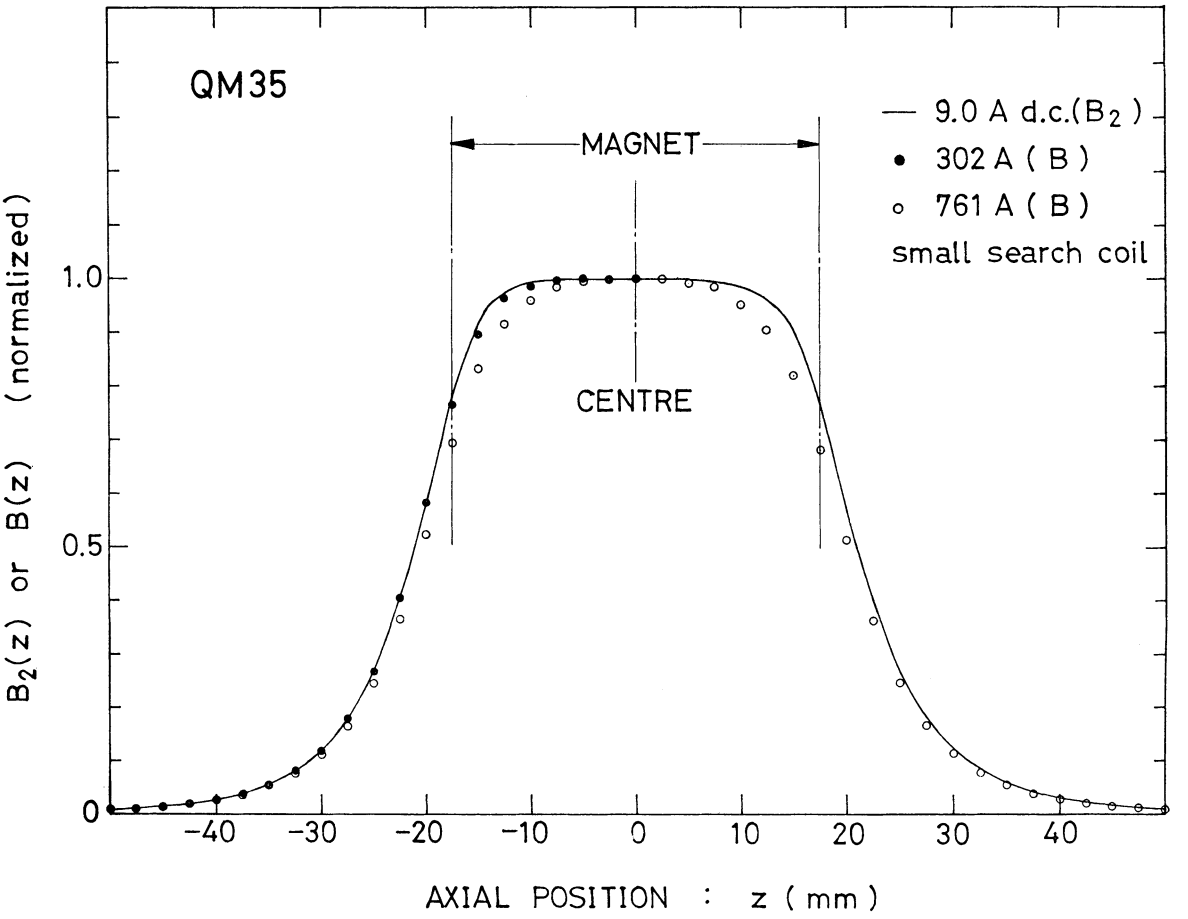

FIG. 13. Fringing field distributions in QM35 at various excitation currents.

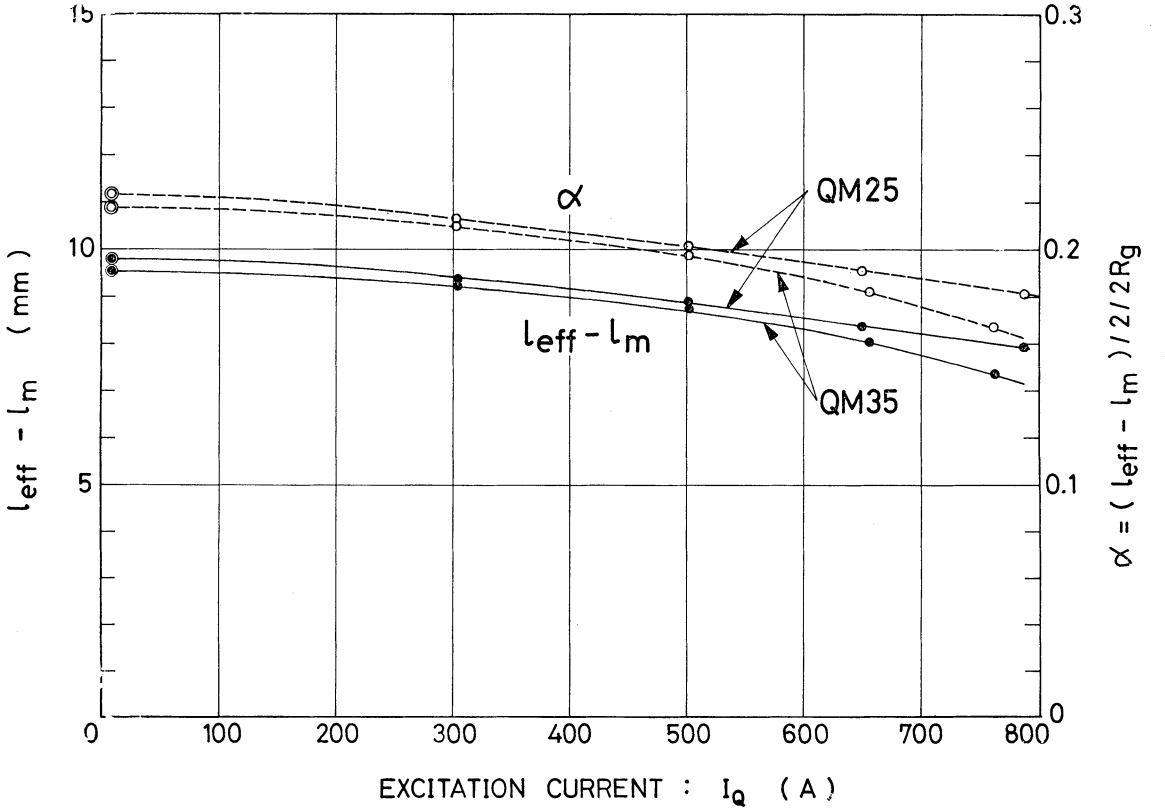

FIG. 14. Effective length of magnet l_{eff} (solid points). Double circles indicate values at the dc excitation of 9.0 A, where the quadrupole component $B_2(z)$ was used instead of $B(z)$ to obtain l_{eff}.

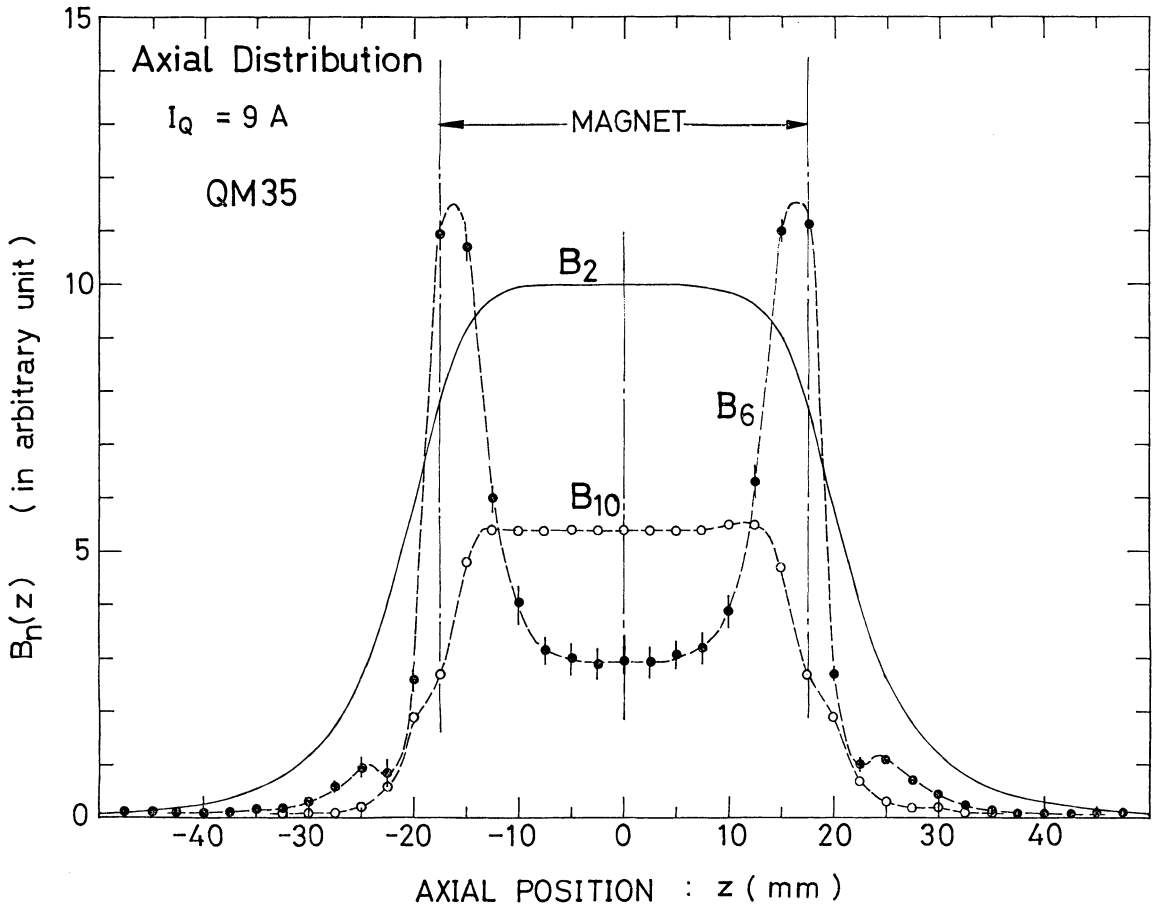

FIG. 15. Fringing field distributions of a QM35 quadrupole magnet. B_n denotes the nth field component. The distribution is presented in an arbitrary unit for each component.

excitation current up to 700 A (the field gradient $\simeq$ 10 kG/cm). With the increasing excitation current, there are trends of a slight increase of the sixth component and of a slight decrease of the tenth one.

The harmonic content was mostly measured with a long coil which included end effects. The obtained quantity corresponds to the actual effect to the beam. The end effects can be separated out by similar measurements with a small search coil. As seen in Fig. 15, the end effects are significant for the term of $n = 6$, while much smaller for $n = 10$.

Eddy Current Effects in Bore Tube[9]

Effects caused by the eddy current in a bore wall of the drift tube can be separated into three parts. First, the eddy current creates an additional magnetic field. Next, as the present power supply[1] uses an inductance–capacitance–resistance resonant circuit, the impedance change due to the eddy current affects both pulse shape and the peak current. Finally, it causes an eddy current loss.

The magnitude of eddy current effects can be expressed in terms of a parameter ε[9] defined as

$$\varepsilon = \frac{\mu_0 \sigma \delta \omega R}{4}\left\{1+\frac{3}{4}\left(\frac{R}{R_g}\right)^4\right\}, \qquad (1)$$

where μ_0 is the permeability of the material, σ the conductivity, δ the wall thickness of the bore tube with an average radius of R and $\omega = \pi/T$.

The bore tube of QM25 was made of stainless steel with $R = 10 \rightarrow 10.4$ mm and $\delta = 0.8$ mm, so ε becomes 0.014 for the present pulse excitation. If the excitation current is fixed, an increase in B_2 is

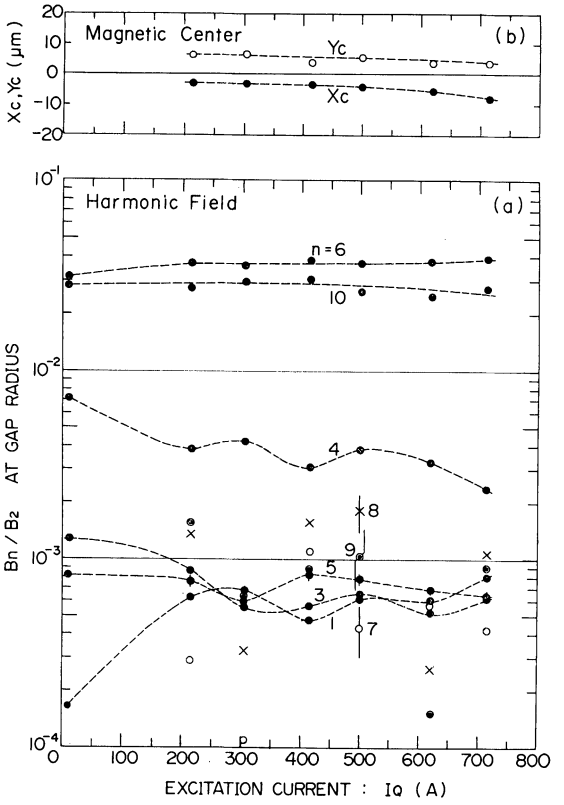

FIG. 16. (a) Harmonic field contents and (b) the magnetic centre versus the excitation current for QM25. For obtaining harmonic contents, the stepping search coil was rotated at a step of five degrees. A dc field measurement at 9.0 A is also given for comparison.

expected to be $\frac{1}{2}\varepsilon^2 \approx 1\times10^{-4}$, which is negligibly small (see Fig. 17). Changes of harmonic contents were negligibly small in agreement with the calculation.[9]

Change of the pulse shape shifts the peak field timing t_0 from the peak excitation current timing t_0'. Agreement between the experiment and the calculation was good as seen in Fig. 18. The difference of t_0-t_0' is proportional to ε, and is about 13 μsec for the present bore tube.

The above results show that all eddy current effects are either negligibly small or can be compensated by readjusting the charging voltage and the timing.

5. CONCLUSION

A field gradient of 11 kG/cm was obtained in drift tube quadrupole magnets of the KEK linac.

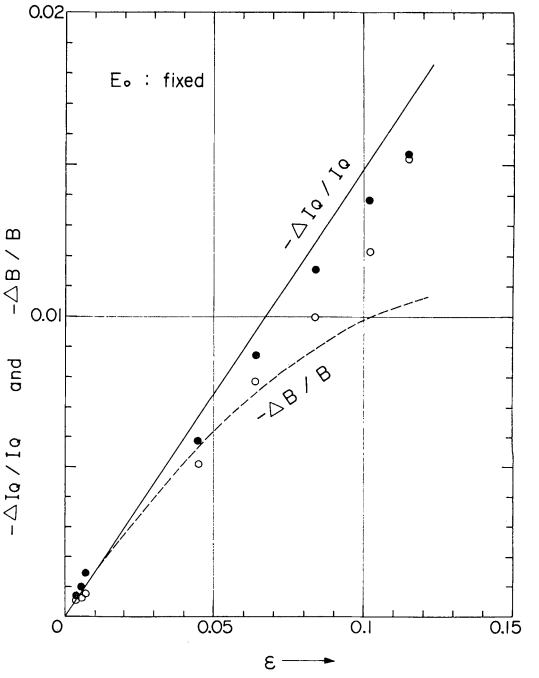

FIG. 17. Measured decreases of B (open circles) and I_Q (solid circles) due to eddy current effects. Curves show the calculation.[9] Charging voltage on the capacitor bank is constant. $T=2.9$ msec.

The 90 magnets were constructed with a tolerance of 20 μm for the difference between the magnetic and the mechanical centres. By virtue of the high mechanical precision of the construction, the bore tube can be easily fitted into the pole gap on the correct mechanical centre of the magnets.

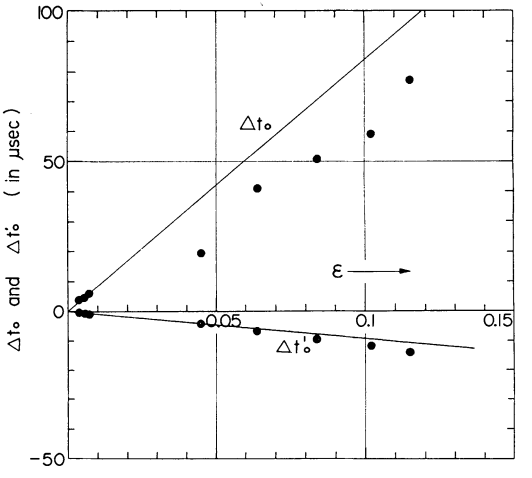

FIG. 18. Shifts of t_0 and t_0' due to eddy current. Solid circles represent experimental results and solid lines a calculation.[9] $T=2.9$ msec.

Measurement of pulsed fields played an important role for establishing the construction method for the magnet. Construction processes should be finally checked by field measurement at actual high field intensity. If the measurement of high intensity pulsed fields were replaced by that of dc fields, a large cooling system would be required, or the measurement would have to be carried out in a short period, with a subsequent wait for the cooling down of the magnet. In these cases, the field measurement would be less convenient and less reliable.

The present measuring system of pulsed fields enabled us to measure saturation characteristics and eddy current effects. The high measuring accuracy also made it possible to study quantitatively small effects such as saturation characteristics at different positions in the pole gap, field intensity dependences of effective length of magnet and harmonic contents, etc.

ACKNOWLEDGEMENTS

The authors express their deep thanks to Professor T. Nishikawa for his useful advice and encouragement throughout the work.

They are grateful to Messrs, S. Ikeda, Y. Fujita, A. Iino and J. Kisaki of Mitsubishi Heavy Industries and Messrs T. Ikeda and M. Nakamori of Tokyo Precision Instruments Co. for their collaboration in the construction of magnets. The present work could not have been achieved without their considerable help in establishing reliable and precise construction processes.

They are also indebted to Professors T. Doke, H. Sasaki and M. Kihara for useful discussions and aids on field measurements.

REFERENCES

1. H. Baba, M. Kobayashi, T. Nishikawa, J. Tanaka, and S. Yamashita, 'Prototype of Drift Tube Quadrupole Magnets', Institute for Nuclear Study Report SJC-A-70-6 (1970).
2. H. Baba, S. Fukomoto, S. Inagaki, M. Kobayashi, T. Nishikawa, S. Okumura, and J. Tanaka, *Proc. 1970 Proton Linear Accelerator Conference, NAL*, p. 35.
3. M. Kobayashi, *Japan. J. Appl. Phys.*, **11,** 47 (1972).
4. M. Kobayashi, J. Tanaka, and S. Yamashita, 'Quality Control for Stacking and Assembling Drift Tube Quadrupole Magnets', National Laboratory for High Energy Physics Report KEK-72-3 (1972).
5. P. Grand, *IEEE Trans. Nucl. Sci.*, **NS-14,** No. 3, 860 (1967).
6. M. Kobayashi, J. Tanaka, H. Baba, and S. Yamashita, *Japan. J. Appl. Phys.*, **10,** 1195 (1971), or Institute for Nuclear Study Report SJC-A-71-1.
7. M. Kobayashi and S. Yamashita, *Nucl. Instr. and Meth.*, **101,** 187 (1972).
8. M. Kobayashi and S. Yamashita, *Nucl. Instr. and Meth.*, **103,** 493 (1972).
9. In preparation for KEK publication.

Received 14 August 1972
and in final form 11 September 1972